Progress in Reaction Kinetics and Mechanism

ARTICLE

Open Access

https://doi.org/10.48130/prkm-0026-0011

Progress in Reaction Kinetics and Mechanism **2026**, 51: e017

Optimizing the gasification performance of corn stover: regulation of the gasification temperature and the equivalence ratio in the lab-scale fixed-bed system

Yanhui Shi[1], Liang Zhu[1], Wei Cai[1], Shengpeng Xia[1], Wenbiao Zhang[1], Weimiao Lu[1], Yutao Zhang[2], Tianfu Zhang[3], Kaige Wang[4*] and Zhongqing Ma[1*]

[1] *Bamboo Industry Institute, Zhejiang A&F University, Hangzhou, Zhejiang 311300, China*
[2] *School of Environment and Resources, Zhejiang A&F University, Hangzhou, Zhejiang 311300, China*
[3] *Institute of Advanced Low-Carbon Technology, State Power Investment Corporation Research Institute Co., Ltd., Beijing 102209, China*
[4] *State Key Laboratory of Clean Energy Utilization, Zhejiang University, Hangzhou, Zhejiang 310007, China*
* Correspondence: kaigewang@zafu.edu.cn (Wang K); mazq@zafu.edu.cn (Ma Z)

Abstract

China has vast reserves of agricultural straw resources. The high-value utilization of agricultural straw through biomass gasification technology holds significant importance for China to achieve 'carbon neutrality' and 'carbon peaking'. This work systematically investigated the effects of equivalence ratio (ER) and gasification temperature (GT) on the properties of the gasified gaseous, solid, and liquid products of corn stover (CS), which was conducted in a home-made and lab-scale fixed-bed gasifier. Results showed that with the increase in GT and ER, the mass yield of bio-gas gradually increased, while the mass yield of bio-char gradually decreased. Higher GT and lower ER were beneficial for improving the lower heating value (LHV) of bio-gas. Specifically, the LHV of bio-gas reached its maximum value of 11.26 MJ/Nm^3 at the GT of 900 °C and the ER of 0.05, along with the contents of H_2, CO, CH_4, and C_nH_m being 22%, 25.91%, 13.59%, and 1.12%, respectively. Furthermore, the contents of H and volatiles in bio-char significantly decreased, while the ash content significantly increased at higher GT and ER. Regarding the tar product, the contents of phenols, alcohols, acids, and aldehydes decreased at higher GT, while the contents of aromatics and ethers increased. In addition, the contents of aromatics and phenols in tar decreased at higher ER, while that of ethers increased.

Citation: Shi Y, Zhu L, Cai W, Xia S, Zhang W, et al. 2026. Optimizing the gasification performance of corn stover: regulation of the gasification temperature and the equivalence ratio in the lab-scale fixed-bed system. *Progress in Reaction Kinetics and Mechanism* 51: e017 https://doi.org/10.48130/prkm-0026-0011

Introduction

In recent decades, the global community has confronted the issue of climate warming caused by excessive CO_2 emissions from fossil fuels. Therefore, production of clean energy and fuels from renewable biomass via thermochemical conversion methods holds significant importance for China in achieving 'carbon neutrality' and 'carbon peaking'[1]. China has vast reserves of agricultural straw resources. The theoretical resource quantity is approximately 829 million tons per year, while the collectible resource quantity is around 694 million tons per year[2]. Currently, the high-value utilization of straw is mainly focused on the following five pathways: fertilizer, feed, fuel, substrate, and industrial raw material. Among these pathways, the biomass gasification technology, which converts agricultural straw into bio-gas, is recognized as an important approach to fulfill the goal of carbon reduction and carbon sequestration[3].

During biomass gasification, solid materials are transformed into gaseous fuels (CO, H_2, CH_4) via a series of thermochemical reactions, including pyrolysis, oxidation, and reduction, driven by gasifying media under elevated temperatures and limited oxygen availability. In addition, gasification also generates two byproducts, namely the biochar and tar[4,5]. The bio-gas can serve as a substitute for the traditional coal and natural gas, which can be applied in the centralized gas supply, the power generation using the internal combustion engine, and the heat supply using boilers[3,6]. The bio-char can be further processed into the activated carbon for the removal of pollutants used in the environmental field, or the bio-char-based fertilizer to improve the yield of crops used in the agricultural field[4,6]. The gasified liquid product is composed of the aqueous part (named as vinegar) and the tar. The vinegar could be used as a disinfectant and a sterilizing agent[7,8].

Biomass gasifiers are typically divided into updraft fixed-bed, downdraft fixed-bed, and fluidized-bed types[3,9]. The downdraft configuration is widely used owing to its low tar output, simple structure, cost advantage, and operational stability[10,11]. In this type of gasifier, pyrolysis volatiles from the upper pyrolysis zone move through the high-temperature oxidation and reduction zones at the bottom. Under elevated temperatures, tar species are further decomposed into lighter combustible gases through secondary cracking reactions, thereby lowering tar content and improving the heating value of the produced gas. Extensive studies have examined how feedstock characteristics, gasification temperature (GT) and equivalence ratio (ER), influence overall gasification performance. Hoque et al.[12] examined how various biomass feedstocks affect gasification performance. Their findings revealed that coconut shell, compared to sawdust and rice husk, produced higher levels of CO, CH_4, and H_2 in the bio-gas, owing to its higher carbon and hydrogen content. Yahaya et al.[13] investigated the influence of GT (700–900 °C) and particle size (1–11 mm) on coconut shell gasification, reporting that smaller particles and higher temperatures enhanced gas production rate and calorific value. Zhu et al.[14] showed that higher ER (0.07–0.16) lowers both gas lower heating value (LHV) and biochar yield. However, the coupled evolution of gas, char, and tar has received comparatively little attention.

In this study, a custom-designed micro-scale fixed-bed reactor was employed to examine how ER and GT influence the gaseous, solid, and liquid products derived from corn stover (CS) (as shown in Fig. 1).

Materials and methods

Feedstock

CS was sourced from Huining County (Baiyin, Gansu, China) and air-dried under ambient conditions. The dried stalks were chopped into 1–3 cm segments and then milled into powder. The resulting material was sieved to obtain particles in the range of 0.075–0.15 mm, followed by oven drying at 105 °C to a constant mass prior to gasification experiments. Analytical methods and product characterization are described in the Supplementary Text 1.

Gasification apparatus and experimental procedure

As illustrated in Fig. 2, gasification experiments were conducted in a self-built micro-scale fixed-bed reactor. The system integrates a gasifier, gas supply unit, feeding module, temperature control unit, cooling circulation system, tar condensation section, and gas collection module. The reactor has an overall height of 800 mm and a width of 300 mm, with a 200 mm heating zone. A quartz reaction tube (40 mm outer diameter, 550 mm length) was employed and electrically heated up to 1,200 °C. The gas supply system includes gas cylinders, mass flow controllers, a flow integrator, and a premixing chamber. The required volumes of N_2 and O_2 were calculated based on different ERs, and their flow rates were regulated by the mass flow controllers. The N_2 and O_2 were premixed before entering the reactor for gasification.

The CS powder was put in a crucible, which was fabricated using the stainless steel plain-weave mesh with a pore size of 0.05 mm. The cooling water circulation system was applied to reduce the temperature of the sealing ring at the top of the quartz tube. A home-made quartz U-tube was placed in a −5 °C ice–salt bath for the tar collection. The gas collection unit consisted of two gas-washing bottles and an aluminum gas bag. The first and second gas-washing bottle were filled with quartz wool and color-changing silica gel, respectively.

Prior to each run, 5 g of CS powder was loaded into the crucible and suspended in the cooling zone of the quartz reactor using a hook. The reactor and pipelines were purged with premixed gasifying agents for 10 min prior to each experiment. The air volume

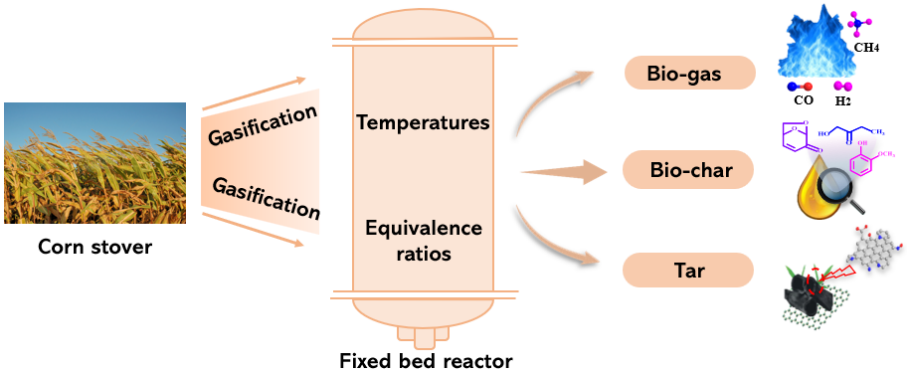

Fig. 1 Schematic illustration of the experimental system employed in this work.

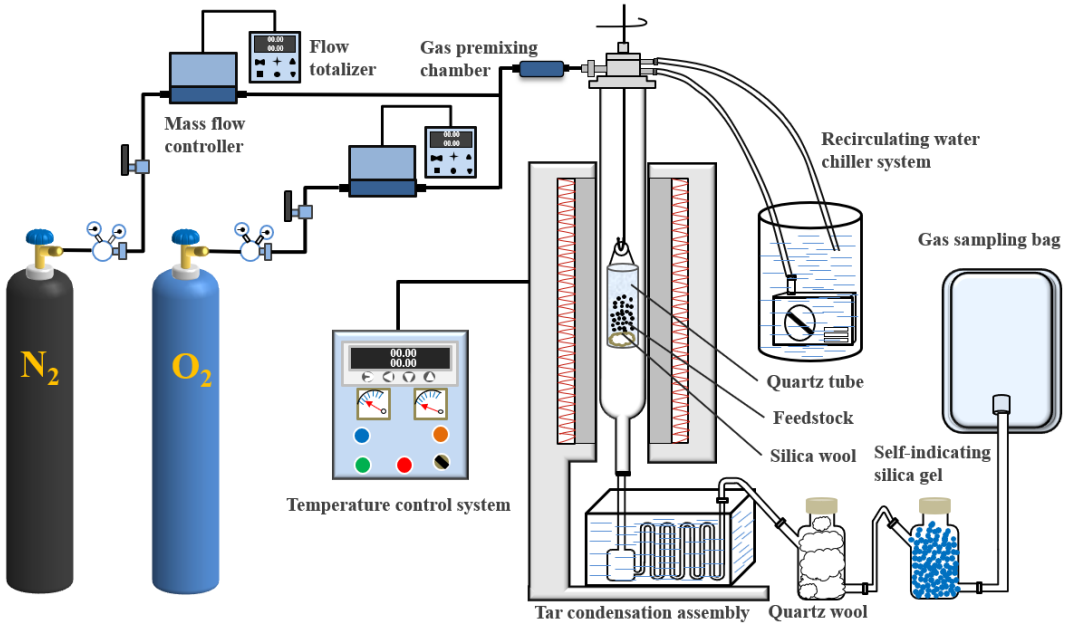

Fig. 2 Configuration of the fixed-bed gasification reactor.

per unit mass of feedstock was calculated using Eq. (1), with ER values of 0.05–0.30. The system was then heated to the target temperature (700, 800, or 900 °C) at 20 °C/min. Once the set temperature was reached, the crucible was rapidly placed into the reaction zone to start gasification, and gas products were collected in a gas bag. After the reaction, the crucible was transferred to the cooling zone and cooled to room temperature. Solid biochar was recovered, gas was collected in the bag, and liquid products were condensed in a U-tube. Bio-char samples obtained under different GT and ER conditions were labeled as CSC-XX-YYY, where CSC denotes CS-derived char, and XX and YYY correspond to ER and GT, respectively. Solid and liquid yields were evaluated using Eqs (2) and (3), while gas yield was obtained by mass balance. Experimental reproducibility was verified through triplicate runs with randomized sampling, and the associated uncertainties are presented as standard deviations.

$$V_{air} = \lambda \frac{22.41}{0.21}\left(\frac{W_C}{12} + \frac{W_H}{4} - \frac{W_O}{32}\right) \quad (1)$$

where, V_{air} represents the air volume (L) required per unit mass of biomass, while W_C, W_H, and W_O correspond to the mass fractions (%) of carbon, hydrogen, and oxygen, respectively.

$$Y_{solid} = \frac{W_{solid}}{W_D} \times 100\% \quad (2)$$

$$Y_{liquid} = \frac{W_{liquid}}{W_D} \times 100\% \quad (3)$$

$$Y_{gas} = 100\% - Y_{solid} - Y_{liquid} \quad (4)$$

where, Y_{solid} and Y_{liquid} represent the yields of the solid and liquid product (%), W_{solid} and W_{liquid} denote the mass (mg) of the bio-char and tar, and W_D is the dry feedstock mass (mg). The yield of gaseous products was calculated by difference, following Eq. (4).

Results and discussion

Effect of GT and ER on the mass yields of gasified products

Figure 3a shows that as GT increased at an ER of 0.05, gas production rose to 59.00% from 48.49%, whereas the liquid and solid fractions declined to 21.12% and 19.89%, respectively. This trend can be attributed to the intensification of devolatilization and oxidation processes at elevated temperatures, which facilitate the conversion of biomass into gaseous products while suppressing char formation[15]. In addition, higher temperatures enhance tar cracking reactions, leading to a reduction in liquid yield[16]. Similar observations have been reported in previous studies; for instance, increasing temperature significantly improved gas yield while reducing char and tar fractions during empty fruit bunch gasification[17]. Moreover, elevated temperatures have been shown to strengthen gas–solid interactions and promote tar reforming reactions, thereby increasing gas yield and reducing tar content[18].

Figure 3b shows that as the ER increased at 900 °C, increasing ER from 0.05 to 0.30 led to a rise in gas yield to 74.91%, accompanied by a sharp reduction in char yield to 5.28%. The tar fraction initially decreased before exhibiting a slight increase at higher ER. This behavior is associated with enhanced oxidation reactions under higher oxygen availability, which accelerate biomass conversion and reduce char formation[19]. Previous studies have reported comparable trends, indicating that elevated ER can promote the formation of tar and oxygenated compounds under certain conditions[20].

Effect of GT and ER on the component distribution and LHV of bio-gas

Figure 4a shows that with increasing GT, the concentrations of H_2, CO, and CH_4 rose to 22.00%, 25.91%, and 13.59% from initial values of 12.08%, 17.46%, and 10.22%, respectively. In contrast, CO_2 and C_nH_m decreased to 6.01% and 1.12% from 12.45% and 1.72%. Correspondingly, the LHV increased to 11.26 from 8.30 MJ/Nm^3. These trends are associated with temperature-dependent reaction pathways. Elevated temperatures enhance devolatilization and oxidation processes, facilitating the formation of permanent gases such as CO, CO_2, CH_4, and H_2. Meanwhile, reduction reactions, including the water–gas shift and Boudouard reactions, are promoted, resulting in increased CO and H_2 and reduced CO_2 concentrations[21–23]. The relatively moderate increase in CH_4 is mainly related to secondary tar cracking and hydrogenation reactions. In addition, the decline in C_nH_m species is attributed to the thermal decomposition of larger hydrocarbons via C–C and C–H bond cleavage, producing lighter gaseous products. Higher temperatures favor CO and H_2 production while inhibiting CO_2 and light hydrocarbons, leading to an improved gas heating value[24].

$$H_2O + C \leftrightarrow CO + H_2 - 131.72\ kJ/mol \quad (5)$$

$$C + CO_2 \leftrightarrow 2CO - 172.43\ kJ/mol \quad (6)$$

$$C + 2H_2 \leftrightarrow CH_4 - 74.8\ kJ/mol \quad (7)$$

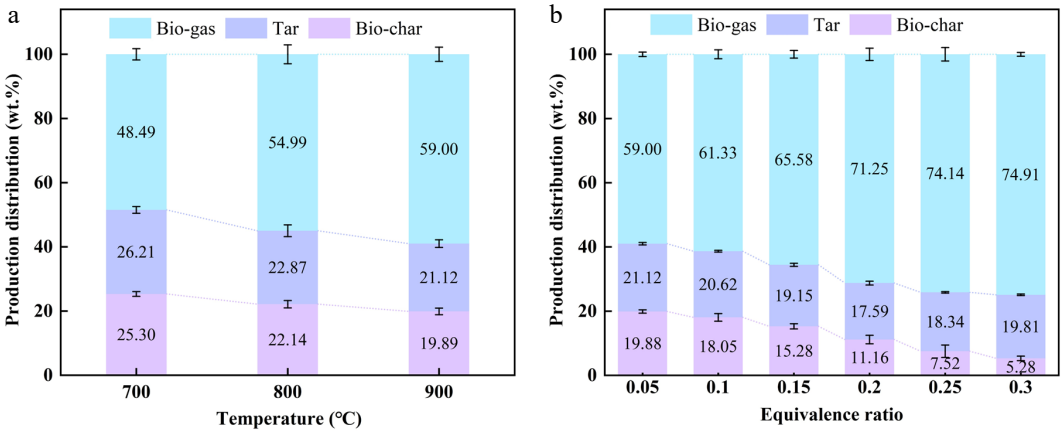

Fig. 3 Effect of (a) GT and (b) ER on the mass yields of gasified products.

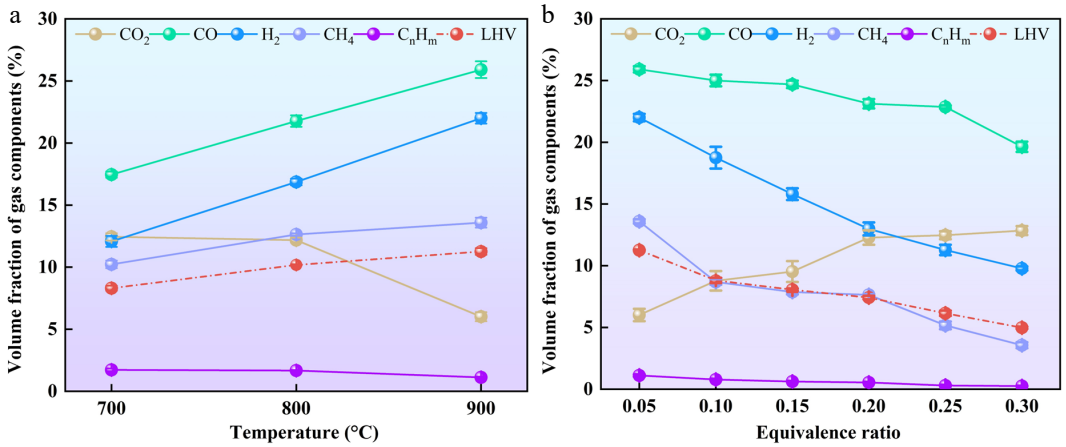

Fig. 4 Effect of (a) GT and (b) ER on the component distribution and LHV of bio-gas.

Figure 4b shows that with increasing ER from 0.05 to 0.30, the concentrations of H_2, CO, CH_4, and C_nH_m decreased to 9.78%, 19.63%, 3.56%, and 0.25% from initial values of 22.00%, 25.91%, 13.59%, and 1.11%, respectively. In contrast, CO_2 increased to 12.85% from 6.01%, while the LHV decreased to 4.98 from 11.26 MJ/Nm^3.

These variations are closely related to the enhanced oxidation environment at higher ER. Increasing ER introduces more oxygen into the reactor, promoting combustion reactions of both bio-char and gaseous species, thereby converting more carbon into CO_2 and H_2O via reactions (8)–(10). In addition, the fraction of N_2 in the product gas increases significantly at higher ER, reaching 63.79% at ER = 0.30, which dilutes the combustible components and leads to a pronounced reduction in LHV. Higher ER suppresses CO, CH_4, and H_2 formation, whereas CO_2 shows a slight increase as oxidation reactions are strengthened[25].

$$C + O_2 \leftrightarrow CO_2 + 393.51\ kJ/mol \quad (8)$$

$$2CO + O_2 \leftrightarrow 2CO_2 + 565.94\ kJ/mol \quad (9)$$

$$CH_4 + 2O_2 \leftrightarrow CO_2 + 2H_2O + 890.36\ kJ/mol \quad (10)$$

Effect of GT and ER on the properties of bio-char

As illustrated in Fig. 5a, increasing temperature from 700 to 900 °C led to an increase in carbon content from 63.74% to 66.25%, while hydrogen and oxygen contents declined to 1.06% and 13.81% from 1.65% and 22.24%, respectively. In addition, volatile matter showed a decreasing trend, whereas ash content increased, accompanied by a slight reduction in fixed carbon. A marginal decline in higher heating value (HHV) was also observed under higher temperature conditions.

As illustrated in Fig. 5b, increasing ER from 0.05 to 0.30 resulted in a pronounced decline in carbon and hydrogen contents. At ER = 0.30, the C and H fractions decreased to 5.36% and 1.01%, respectively. Meanwhile, volatile matter and fixed carbon were substantially reduced, whereas ash content increased markedly, reaching 70.43%. These results indicate that under severe gasification conditions (ER = 0.30, GT = 900 °C), bio-char is extensively converted into ash. When ER exceeds 0.25, the ash content surpasses 70%, leading to a significant deterioration in HHV.

Effect of GT and ER on the composition of gasified liquid product

Figure 6 presents the total ion chromatography of the gasified liquid product obtained at different GTs and ERs. The detailed component of the gasified liquid product is presented in Supplementary Tables S1 and S2. The organic components of the liquid products can be classified into nine groups, including the acids, esters, aromatic hydrocarbons, aldehydes, ketones, alcohols, phenols, furans, and other aliphatic hydrocarbons.

As shown in Fig. 7a, with increasing GT from 700 to 900 °C, the acid fraction decreased from 4.8% to nearly zero, which is attributed

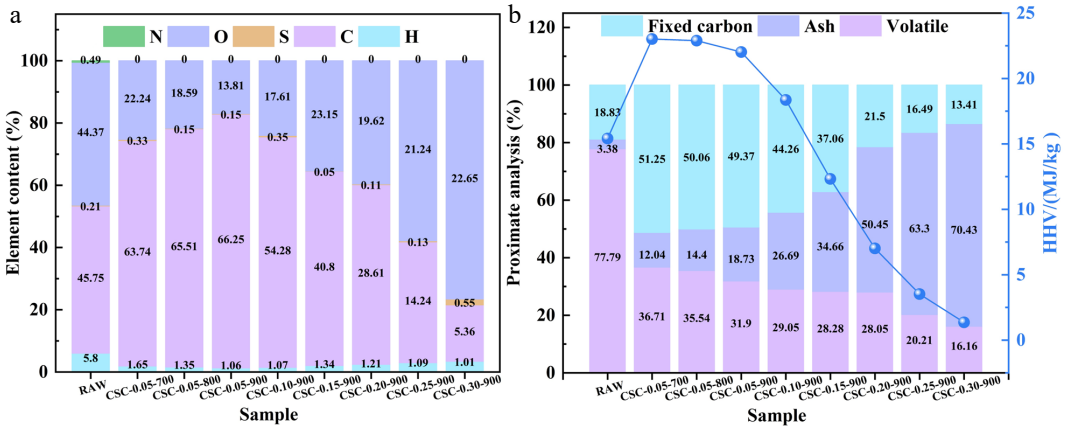

Fig. 5 Effect of (a) GT and (b) ER on the basic properties of biochar.

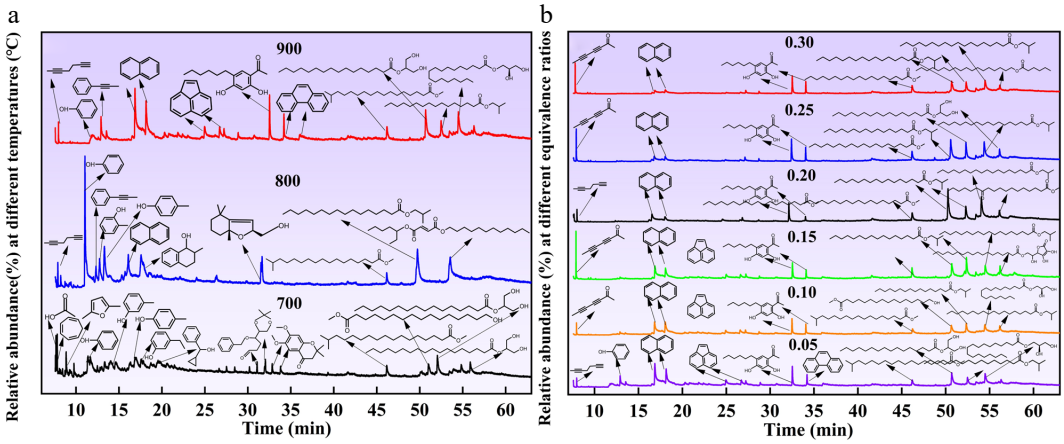

Fig. 6 The total ion chromatography of the gasified liquid product obtained at different (a) GTs and (b) ERs.

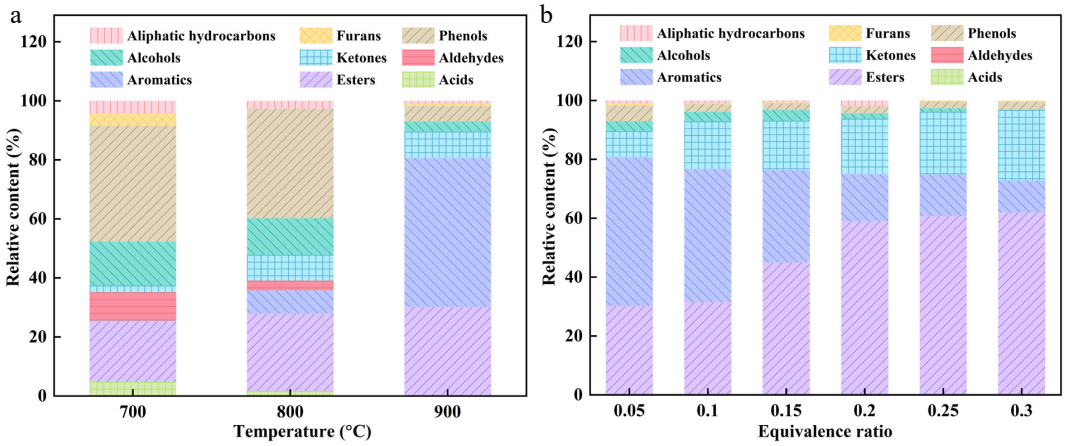

Fig. 7 Effect of (a) GT and (b) ER on the compound distribution of the gasified liquid product.

to enhanced secondary cracking reactions that convert acids into other organic species[26]. In contrast, esters and ketones increased to 30.2% and 8.87% from initial values of 20.45% and 2.29%, respectively. Meanwhile, alcohols, aldehydes, and furans decreased to 3.4%, 0%, and 0.77% from 14.82%, 9.60%, and 4.07%, respectively.

These variations are closely associated with the thermal decomposition behavior of biomass components. The formation of ketones and the decline of furans and aldehydes are mainly governed by ring-opening and depolymerization reactions of hemicellulose and cellulose, which are intensified at elevated temperatures[27]. In addition, phenols decreased markedly from 39.29% to 5.26% due to enhanced deoxygenation and aromatization reactions[28]. Conversely, aromatic hydrocarbons exhibited a substantial increase, reaching 50.5% from 0.32%, as a result of the progressive deoxygenation of oxygenated intermediates in tar[23,28]. Similar observations have been reported in previous studies, where increasing temperature promotes the conversion of tar components into aromatic hydrocarbons such as indene and naphthalene[29].

As shown in Fig. 7b, with increasing ER from 0.05 to 0.30, the ester fraction rose to 61.9% from 30.2%, whereas alcohols declined markedly to 0.12% from 3.4%, which is associated with the suppression of alcohol formation under higher oxygen availability. Previous studies have demonstrated that operating parameters such as ER play a critical role in tar formation and the distribution of oxygenated compounds during biomass gasification[30–32].

In addition, ketones exhibited an overall increase, reaching 24% from 8.87%, while furans showed a decreasing tendency, remaining at low levels (0.77% to 0.46%). The phenol content decreased from 5.26% and stabilized at approximately 2% with further increases in ER. In contrast, aromatic hydrocarbons declined significantly, dropping to 10.83% from 50.5%, which can be attributed to enhanced oxidation reactions between aromatic species and oxygen under higher ER conditions[33,34].

Conclusions

This study examines the gasification behavior of CS in a lab-scale fixed-bed reactor, with particular emphasis on the effects of GT and ER on the distribution and properties of gaseous, solid, and liquid products. The main conclusions are summarized as follows:

(1) Both GT and ER exert a strong influence on product distribution. Increasing these parameters promotes gas formation while suppressing biochar yield.

(2) GT and ER play a critical role in determining gas quality. Raising the temperature from 700 to 900 °C increases the LHV from 8.30 to 11.26 MJ/Nm^3, whereas increasing ER from 0.05 to 0.30 leads to a significant decline in LHV from 11.26 to 4.98 MJ/Nm^3.

(3) Elevated GT and ER adversely affect bio-char quality, resulting in reduced carbon, hydrogen, and volatile contents, accompanied by a substantial increase in ash content.

(4) Higher temperatures favor the formation of aromatic compounds in liquid products, whereas increasing ER suppresses aromatic formation, leading to a gradual decline in their abundance.

Author contributions

The authors confirm contribution to the paper as follows: study conception and design: Zhang W, Lu W, Zhang Y, Zhang T, Wang K, Ma Z; investigation: Shi Y; software: Zhu L, Cai W, Xia S; visualization: Zhu L, Cai W, Xia S; resources: Zhang W, Lu W, Zhang Y, Zhang T; draft manuscript preparation: Shi Y; writing – review & editing: Wang K, Ma Z; supervision: Zhang W, Lu W, Zhang Y, Zhang T, Wang K, Ma Z. All authors reviewed the results and approved the final version of the manuscript.

Data availability

All data generated or analyzed during this study are included in this published article and its supplementary information files.

Acknowledgments

This research was supported by the 'Pioneer' and 'Leading Goose' R&D Program of Zhejiang Province (Grant Nos 2025C01173, 2024C03225), the National Natural Science Foundation of China (Grant No. 52376214).

Conflict of interest

The authors declare that they have no known competing financial interests or personal relationships that could have appeared to influence the work reported in this paper.

Supplementary information accompanies this paper online at: https://doi.org/10.48130/prkm-0026-0011.

Dates

Received 4 November 2025; Revised 15 February 2026; Accepted 24 March 2026; Published online 9 June 2026

References

[1] Wei J, Wang M, Wang F, Song X, Yu G, et al. 2021. A review on reactivity characteristics and synergy behavior of biomass and coal Co-gasification. *International Journal of Hydrogen Energy* 46:17116–17132

[2] Zhang DY, Liu HR, Wang Y. 2021. *Blue book on the development potential of carbon-neutral biomass energy under the 30·60 dual-carbon targets*. https://huanbao.bjx.com.cn/news/20210915/1177039.shtml

[3] Ma Z, Zhang Y, Zhang Q, Qu Y, Zhou J, et al. 2012. Design and experimental investigation of a 190 kWe biomass fixed bed gasification and polygeneration pilot plant using a double air stage downdraft approach. *Energy* 46:140–147

[4] Heidenreich S, Foscolo PU. 2015. New concepts in biomass gasification. *Progress in Energy and Combustion Science* 46:72–95

[5] Bai Z, Liu Q, Lei J, Li H, Jin H. 2015. A polygeneration system for the methanol production and the power generation with the solar–biomass thermal gasification. *Energy Conversion and Management* 102:190–201

[6] Ma Z, Chen D, Gu J, Bao B, Zhang Q. 2015. Determination of pyrolysis characteristics and kinetics of palm kernel shell using TGA–FTIR and model-free integral methods. *Energy Conversion and Management* 89:251–259

[7] Gama GSP, Santos Pimenta A, Feijó FMC, Aires CAM, de Melo RR, et al. 2024. Antimicrobial impact of wood vinegar produced through co-pyrolysis of eucalyptus wood and aromatic herbs. *Antibiotics* 13:1056

[8] Gama GSP, Santos Pimenta A, Feijó FMC, de Azevedo TKB, de Melo RR, et al. 2024. The potential of wood vinegar to replace antimicrobials used in animal husbandry – a review. *Animals* 14:381

[9] Sansaniwal SK, Pal K, Rosen MA, Tyagi SK. 2017. Recent advances in the development of biomass gasification technology: a comprehensive review. *Renewable and Sustainable Energy Reviews* 72:363–384

[10] Martínez LV, Rubiano JE, Figueredo M, Gómez MF. 2020. Experimental study on the performance of gasification of corncobs in a downdraft fixed bed gasifier at various conditions. *Renewable Energy* 148:1216–1226

[11] Trejo F. 2025. Review of biomass gasification technologies with a particular focus on a downdraft gasifier. *Processes* 13:2717

[12] Hoque ME, Rashid F, Aziz M. 2021. Gasification and power generation characteristics of rice husk, sawdust, and coconut shell using a fixed-bed downdraft gasifier. *Sustainability* 13:2027

[13] Yahaya AZ, Somalu MR, Muchtar A, Sulaiman SA, Wan Daud WR. 2019. Effect of particle size and temperature on gasification performance of coconut and palm kernel shells in downdraft fixed-bed reactor. *Energy* 175:931–940

[14] Zhu D, Wang Q, Xie G, Ye Z, Zhu Z, et al. 2024. Effect of air equivalence ratio on the characteristics of biomass partial gasification for syngas and biochar co-production in the fluidized bed. *Renewable Energy* 222:119881

[15] Situmorang YA, Zhao Z, Yoshida A, Abudula A, Guan G. 2020. Small-scale biomass gasification systems for power generation (<200 kW class): a review. *Renewable and Sustainable Energy Reviews* 117:109486

[16] Ren J, Cao JP, Zhao XY, Yang FL, Wei XY. 2019. Recent advances in syngas production from biomass catalytic gasification: a critical review on reactors, catalysts, catalytic mechanisms and mathematical models. *Renewable and Sustainable Energy Reviews* 116:109426

[17] Mohammed MAA, Salmiaton A, Wan Azlina WAKG, Mohammad Amran MS, Fakhru'l-Razi A. 2011. Air gasification of empty fruit bunch for hydrogen-rich gas production in a fluidized-bed reactor. *Energy Conversion and Management* 52:1555–1561

[18] Gálvez-Pérez A, Martín-Lara MA, Calero M, Pérez A, Canu P, et al. 2021. Experimental investigation on the air gasification of olive cake at low temperatures. *Fuel Processing Technology* 213:106703

[19] Martínez JD, Mahkamov K, Andrade RV, Silva Lora EE. 2012. Syngas production in downdraft biomass gasifiers and its application using internal combustion engines. *Renewable Energy* 38:1–9

[20] Horvat A, Pandey DS, Kwapinska M, Mello BB, Gómez-Barea A, et al. 2019. Tar yield and composition from poultry litter gasification in a fluidised bed reactor: effects of equivalence ratio, temperature and limestone addition. *RSC Advances* 9:13283–13296

[21] Jarungthammachote S, Dutta A. 2012. Experimental investigation of a multi-stage air-steam gasification process for hydrogen enriched gas production. *International Journal of Energy Research* 36:335–345

[22] Lyons Cerón A, Konist A, Lees H, Järvik O. 2021. Effect of woody biomass gasification process conditions on the composition of the producer gas. *Sustainability* 13:11763

[23] Ma Z, Ye J, Zhao C, Zhang Q. 2015. Gasification of rice husk in a downdraft gasifier: the effect of equivalence ratio on the gasification performance, properties, and utilization analysis of byproducts of char and tar. *Bioresources* 10:2888–2902

[24] Hernández JJ, Aranda G, Barba J, Mendoza JM. 2012. Effect of steam content in the air–steam flow on biomass entrained flow gasification. *Fuel Processing Technology* 99:43–55

[25] Al-Farraji A, Marsh R, Steer J, Valera-Medina A. 2019. Kinetics and performance of raw and torrefied biomass in a continuous bubbling fluidized bed gasifier. *Waste and Biomass Valorization* 10:1365–1381

[26] Shen D, Zhang L, Xue J, Guan S, Liu Q, et al. 2015. Thermal degradation of xylan-based hemicellulose under oxidative atmosphere. *Carbohydrate Polymers* 127:363–71

[27] Chen D, Gao A, Cen K, Zhang J, Cao X, et al. 2018. Investigation of biomass torrefaction based on three major components: hemicellulose, cellulose, and lignin. *Energy Conversion and Management* 169:228–237

[28] Cortazar M, Alvarez J, Lopez G, Amutio M, Santamaria L, et al. 2018. Role of temperature on gasification performance and tar composition

in a fountain enhanced conical spouted bed reactor. *Energy Conversion and Management* 171:1589–1597

[29] Feng D, Zhao Y, Zhang Y, Sun S. 2017. Effects of H_2O and CO_2 on the homogeneous conversion and heterogeneous reforming of biomass tar over biochar. *International Journal of Hydrogen Energy* 42:13070–13084

[30] Milne TA, Abatzoglou N, Evans RJ. 1998. Biomass gasifier 'tars': their nature, formation, and conversion. *Report No. NREL/TP-570-25357*. National Renewable Energy Laboratory, Golden, CO, USA. doi: 10.2172/3726

[31] Phuphuakrat T, Nipattummakul N, Namioka T, Kerdsuwan S, Yoshikawa K. 2010. Characterization of tar content in the syngas produced in a downdraft type fixed bed gasification system from dried sewage sludge. *Fuel* 89:2278–2284

[32] Kinoshita CM, Wang Y, Zhou J. 1994. Tar formation under different biomass gasification conditions. *Journal of Analytical and Applied Pyrolysis* 29:169–181

[33] Ledesma EB, Kalish MA, Nelson PF, Wornat MJ, Mackie JC. 2000. Formation and fate of PAH during the pyrolysis and fuel-rich combustion of coal primary tar. *Fuel* 79:1801–1814

[34] Phuphuakrat T, Namioka T, Yoshikawa K. 2010. Tar removal from biomass pyrolysis gas in two-step function of decomposition and adsorption. *Applied Energy* 87:2203–2211